Journal of Soils and Sediments (2023) 23:1607–1616
https://doi.org/10.1007/s11368-023-03433-x

SOILS, SEC 1 • SOIL ORGANIC MATTER DYNAMICS AND NUTRIENT CYCLING • RESEARCH ARTICLE

The remediation of hexavalent chromium-contaminated soil by nanoscale zero-valent iron supported on sludge-based biochar

Xi Chen[1] · Guangjian Fan[1,2] · Xiaoxuan Zhu[1] · Haibo Li[1] · Yinghua Li[1] · Hui Li[3] · Xinyang Xu[1,2]

Received: 29 April 2022 / Accepted: 11 January 2023 / Published online: 19 January 2023

Abstract

Purpose This research investigates the capability of biochar (BC)–supported nanoscale zero-valent iron (nZVI) composite (nZVI/BC) with strong adsorption and reduction properties for immobilization of hexavalent chromium (Cr(VI)) in Cr(VI)-polluted soil.

Methods Liquid phase reduction method was used to prepare nZVI and nZVI/BC. Cr-contaminated soils were amended with BC, nZVI, and nZVI/BC. Toxicity characteristic leaching procedure (TCLP)–leachable Cr(Cr(VI)) was measured to evaluate the immobilization efficiency by three materials. The sequential extraction procedure (SEP) method was applied for Cr fraction analysis. The changes of soil properties and the reaction mechanism between Cr(VI) and nZVI/BC were also analyzed.

Results and discussion NZVI/BC exhibited a superior capacity for reducing TCLP-leachable Cr(VI) than nZVI and BC. The fraction analysis suggested that nZVI/BC could effectively reduce the toxicity of Cr(VI) by promoting the transformation of more accessible forms (exchangeable (EX)) into less accessible forms (iron-manganese oxides-bound (OX)). Compared with nZVI, the addition of BC and nZVI/BC could improve soil properties during a short term. X-Ray photoelectron spectroscopy (XPS) analysis showed that the redox reaction might be the main reaction mechanism between Cr(VI) and nZVI/BC.

Conclusion NZVI/BC exhibited superior remediation capacity for Cr(VI)-polluted soil due to its high reduction and adsorption capacity. Moreover, those nano-particles could be recovered by magnetic separation after remediation process, and the recovery rate could reach more than 60%. Hence, nZVI/BC had a valuable utilization for the immobilization of Cr(VI) in soil.

Keywords Biochar · Nanoscale zero-valent iron · Cr(VI)-polluted soil · Magnetic separation · Fe(III)–Cr(III) coprecipitant

1 Introduction

Over the years, due to human and industrial activities, soils have been contaminated by heavy metals (HMs) (Tu et al. 2020). HMs are generally highly toxic and undegradable in the environment, which makes them a huge threat to humans and ecosystems (Geng and Wang 2019). As a common HM element, chromium (Cr) is widely abundant in soil environment (Megharaj et al. 2003). Among the several chemical species of Cr, trivalent chromium (Cr(III)) and Cr(VI) are the relatively stable oxidation states of Cr that exist in soil medium (Kotaś and Stasicka 2000). Compared with Cr(III), Cr(VI) is far more harmful to human health due to its high toxicity (Shi et al. 2011).

Various treatment technologies, such as phytoremediation, microbial remediation, and soil washing, have been applied for soil remediation (Sarwar et al. 2017). However, these technologies have low remediation efficiency and are expensive (Wang et al. 2021). Being a material prepared by pyrolysis technology (heating under high temperature with little or no oxygen), Biochar (BC) has strong adsorption capacity due to its unique pore structure and various surface functional groups, which can be applied for HMs removal (Ahmed et al. 2021). Nowadays, many researchers focused on the modification of BC, especially the synthesize

Responsible editor: Xilong Wang.

✉ Xinyang Xu
Xuxinyang202102@163.com

[1] School of Resources and Civil Engineering, Northeastern University, Shenyang 110819, China

[2] Foshan Graduate School of Northeastern University, Foshan 528311, China

[3] Shenyang Ecological Environment Affairs Service Center Helping Branch Center, Shenyang 110006, China

of BC-based nanocomposites which combines the advantages of BC with nano-materials (Tan et al. 2016).

Nanoscale zero-valent iron (NZVI) is effective in the treatment of Cr in aqueous system (Liu et al. 2009). Due to its strong reducing ability, the toxic Cr(VI) can be converted to non-toxic Cr(III) (Singh et al. 2011). However, the agglomeration effect of nZVI particles is strong due to its magnetic interaction, and it is easily oxidized (Xu and Zhao 2007). Using BC as a carrier of nZVI to synthesize a new material has been documented by several researchers (Miao et al. 2021; Su et al. 2016). The specific structure and unique surface property of BC makes it an outstanding supporting material to prevent agglomeration of nZVI, which enhances the stability of nZVI particles, thereby increasing its remediation efficiency (Devi and Saroha 2014). Over years, NZVI/BC had been used for Cr(VI) removal in aqueous system, while there are still a few research on remediation of Cr(VI)-polluted soil by nZVI/BC.

In our study, pyrolysis from municipal sewage sludge (MSS) was applied to prepare BC. Liquid phase reduction method was used to prepare nZVI/BC. This study aimed to (1) evaluate the potentials of nZVI/BC for the remediation of Cr-contaminated soil and (2) explore the reaction mechanism between nZVI/BC and Cr(VI).

2 Materials and methods

2.1 Synthesis of remediation materials

MSS was collected from municipal wastewater treatment plants in China. The process of BC preparation was as follows: At first, the MSS was soaked in zinc chloride ($ZnCl_2$) solution for 24 h to increase the pore structure of BC. After that, the materials were dried and ground to 1 mm, then the MSS was heated inside the pyrolysis furnace at 600 °C for 60 min under nitrogen (N_2) conditions. Finally, the product was washed with deionized water (DI) to remove the surface impurities (Xi et al. 2021). The pH of BC was measured at a soil/water ratio of 1:20 (Ruili et al. 2020). An element analyzer (Vario MACRO cube, Germany) was used to determine the total C, O, N, H, and S contents of BC. The ash content of BC was measured by an industrial analyzer (TRGF-8000, China). The properties of BC are shown in Table 1.

nZVI/BC was prepared by liquid phase reduction method. In brief, 2.8 g of BC was put into $FeSO_4 \cdot 7H_2O$ solution (100 mL) of 0.25, 0.5, and 1.0 M, separately, and stirred in nitrogen for 4 h. Afterward, $NaBH_4$ solution (100 mL, 2.0 M), which is a strong reducing agent, was added dropwise to the reactor under nitrogen (N_2) atmosphere. After the reaction, the prepared materials were separated from the reactor and washed with ethanol several times, so as to prevent the oxidation of nZVI. The nanomaterials were vacuum dried at 60 °C before further experiment.

Table 1 Properties of BC

Properties	BC
PH	8.52
C (%)	36.30
H (%)	3.41
O (%)	17.25
N (%)	3.56
S (%)	0.90
Ash (%)	29.29

2.2 Soil sample preparation

The Cr(VI)-free soil samples were collected at 0–20 cm depth from former nonferrous metals processing factory in Shenyang, China. To prepare a Cr(VI)-spiked soil, 1 L of $K_2Cr_2O_7$ solution (500 mg/L) was mixed with 1 kg of air-dried soil and mixed for 2 weeks with a 50% moisture content, then stirred until the mixture was air dried to a constant weight (Su et al. 2016). The physicochemical properties of the soil are shown in Table 2.

2.3 Remediation experiments

Initially, nZVI/BC materials with three different nZVI loads (107.1, 282.1, and 407.4 mg/g) were added to the Cr(VI)-contaminated soil (500 g). The mixtures were immobilized with a moisture content of 50% under room temperature and samples were taken at 5, 15, 30, and 45 days. Toxicity characteristic leaching procedure (TCLP) test was applied for estimating the efficiency of the nZVI/BC on Cr immobilization. The Cr(VI) immobilization efficiency was calculated according to Eq. (1):

$$E_i = \frac{C_o - C_i}{C_o} \times 100\% \quad (1)$$

where E_i is the Cr (Cr(VI)) stabilization efficiency in the soil sample, and C_o and C_i are the initial and final concentration of TCLP-extractable Cr(VI), respectively, in the soil. Untreated soils were taken as control and all treatments were set up in three groups of parallel experiments. The optimal nZVI loads and remediation time were selected for further experiment.

Afterward, the Cr(VI) remediation capabilities of BC, nZVI, and nZVI/BC were analyzed. The nZVI/BC dose were set as 2, 4, and 8 g/kg, respectively, whereas the nZVI and BC dose were based on nZVI loads (Fe content) and BC content of nZVI/BC particles, separately. The soil remediation condition was as described above. The leachability of Cr (Cr(VI))

Table 2 Properties of the soil samples

Sample	PH	CEC (cmol/kg)	SOM (g/kg)	Fe (g/kg)	Cr (mg/kg)	Cr(VI) (mg/kg)
Cr-free soil	6.48	6.55	11.14	23.8	141.0	ND
Cr(VI)-spiked soil	6.73	6.59	10.72	23.0	533.7	323.0

and Fe were tested by TCLP methods as well. The Cr(Fe) or Cr(VI) content in soil samples were analyzed via acid or alkaline digestion method and determined by atomic absorbance spectrometry (AAS, Z-2300, Japan). The fraction analysis of Cr followed a sequential extraction procedure (SEP) developed by Tessier (Lyu et al. 2018). The order of the extraction was exchangeable (EX) > carbonate-bound (CB) > iron-manganese oxides-bound (OX) > organic material-bound (OM) > residual (RS). Moreover, the soil pH, soil organic matter (SOM), and cation exchange capacity (CEC) were determined before and after remediation process according to the methods of previous research (Ruili et al. 2020). The soil pH was measured by potentiometric method with a soil/water ratio of 1:2.5. The SOM was determined by using wet oxidation with H_2SO_4-$K_2Cr_2O_7$. Moreover, the CEC was determined by ammonium acetate (NH_4OAc) method.

2.4 Separation and characterization methods

After the incubation process, 100 g of soil sample was air dried and ground to 200 mesh, then the nZVI/BC particles were separated by using a magnet; the separated particles were washed with ethanol several times and vacuum dried at 60 °C before analysis.

Inductively coupled plasma–optical emission spectroscopy (ICP-OES, Avio 500, USA) was applied for testing the Fe content of remediation materials. Scanning electron microscopy (SEM; Zeiss Sigma 300, Germany) and energy-dispersive X-ray spectroscopy (EDS) were used for investigating the morphology of nanomaterials. The crystal structures of BC and nZVI/BC were characterized by X-ray diffraction (XRD; Rigaku Ultima IV, Japan). The surface functional groups of BC and nZVI/BC were characterized by Fourier-transform infrared spectroscopy (FTIR; Nicolet iS 10, USA). X-Ray photoelectron spectroscopy (XPS; Thermo Scientific K-Alpha$^+$, USA) was used for characterization of nZVI/BC.

2.5 Statistical analysis

IBM SPSS Statistics for Windows version 25 (IBM Corp., Armonk, N.Y., USA) was used for the statistical analysis. Data were analyzed by one-way analysis of variance with Duncan's multiple range post hoc test ($p < 0.05$). All figures were produced by Origin 2018.

3 Results and discussion

3.1 Effect of nZVI loads (Fe content) and remediation time

The Cr(VI) immobilization efficiency was 44.23%, 53.32%, and 76.01% at 30 days and were 107.1, 282.1, and 407.4 mg/g, respectively, under the nZVI loads in nZVI/BC (each group contain same mass of BC) (Fig. 1). Afterwards, the TCLP-extractable Cr(VI) was almost unchanged. The results showed that the nZVI loads influenced the immobilization efficiency due to the reactive sites increased with the increase of nZVI loads. During the remediation process, the nZVI particles was gradually oxidized and finally lost its reactivity. Therefore, the optimal nZVI loads and remediation time were selected as 407.4 mg/g and 30 days for the next experiment.

3.2 Comparison of immobilization efficiency by BC, nZVI, and nZVI/BC

3.2.1 TCLP extraction analysis

TCLP test was used to evaluate the Cr (Cr(VI)) immobilization efficiency of three materials. Figure 2 shows the TCLP-leachable Cr (Cr(VI)) and Fe concentrations in the untreated and treated soils. As shown in Fig. 2a, b, the Cr and Cr(VI)

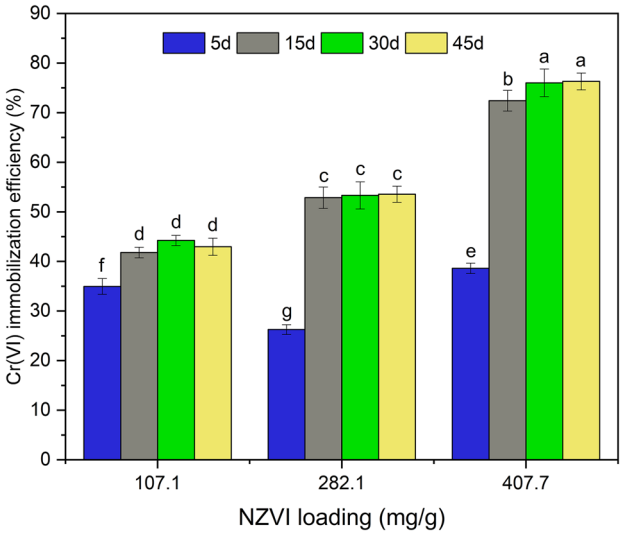

Fig. 1 Effect of nZVI loads and remediation time on Cr(VI) immobilization efficiency

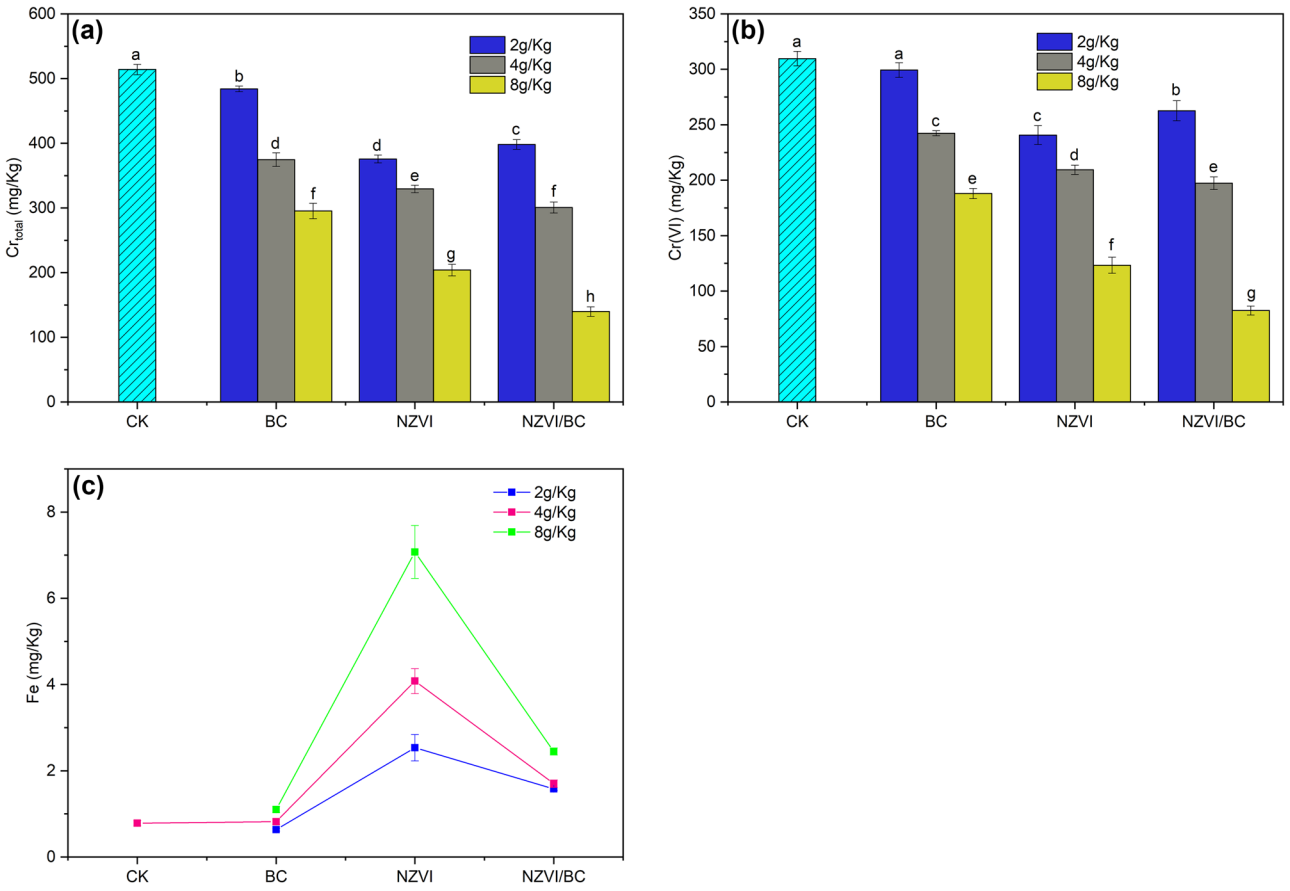

Fig. 2 TCLP-extractable Cr, Cr(VI), and Fe in soil with different treatment methods (**a**–**c**)

concentrations in TCLP leachates were 514.0 and 309.7 mg/kg in the contaminated soil. The changes in TCLP-leachable Cr or Cr(VI) decreased with higher dose for each of the remediation materials. The use of BC reduced TCLP-leachable Cr(VI) from 309.7 to 188.0 mg/kg under the maximum dosage. For the nZVI-treated soil, the immobilization efficiency for Cr(VI) was 60.19%, which was much higher than that of BC. The nZVI/BC treatment exhibited superior performance for Cr(VI) remediation. After nZVI/BC treatment, the TCLP-leachable Cr(VI) reduced from 309.7 to 262.7, 197.3, and 82.5 mg/kg under the dose of 2, 4, and 8 g/kg, respectively. The result showed that compared with BC, nZVI was high effective for Cr(VI) immobilization in the short term, which was due to the strong reducing ability of nZVI. However, as a supporting material, BC played a significant role in preventing the agglomeration effect of nZVI, thus endowing the nZVI/BC with stronger immobilization efficiency for Cr(VI).

The proper amount of iron was helpful for the growth of soil microorganisms and plants (Xiaoyan et al. 2022). As shown in Fig. 2c, compared with the contaminated soil and the BC-treated soil, the TCLP-leachable Fe for nZVI or nZVI/BC-treated soil increased significantly, which might be caused by the excessive release of iron in the soil system during the immobilization procedure (Sneath et al. 2013). However, as a carrier, BC can improve the stability of iron in a reaction system, thereby reducing the release of iron (Devi and Saroha 2014).

3.2.2 Cr fraction analysis

To further explore the immobilization efficiency of Cr(VI) by three materials, the fraction transformation of Cr before and after remediation was investigated (Fig. 3). Cr species in the contaminated soil were EX (37.78%), CB (20.79%), OX (10.91%), OM (21.89%), and RS (8.63%). Among them, the EX and CB were the most available form of Cr. After BC treatment, EX and CB both decreased to 20.11% and 17.25%, respectively, whereas OX, OM, and RS increased to 26.96%, 26.47%, and 9.22%, respectively. The well-developed pore structure and the abundant oxygen-containing functional groups on the surface of biochar endowed BC with strong adsorption capacity, thereby decreasing the more accessible forms of Cr. Cr species in the nZVI-treated soil were as follows: CB (13.00%), OM (21.56%), and RS (8.56%). Compared with BC, EX fraction decreased to 14.99%, whereas

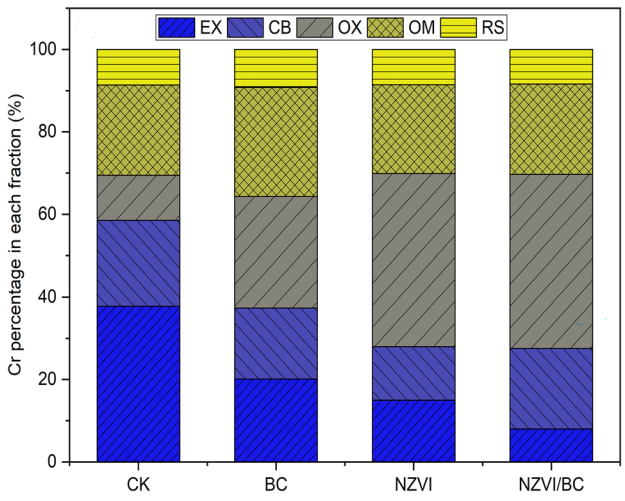

Fig. 3 The changes in Cr fraction before and after remediation

OX remarkably increased to 41.89%. For nZVI/BC-treated soil, the speciation transformation of Cr was almost the same as that of nZVI-treated soil. The EX fraction decreased to 8.03% and the OX fraction increased to 42.18%. As we reported in a previous research, the Fe(III)–Cr(III) coprecipitant could be formed during the reaction between Cr(VI) and nZVI/BC (Xi et al. 2021). The formation of Cr(III)/Fe(III) oxides/hydroxides might contribute to the increase in OX fraction (Manning et al. 2007). The result implied that both nZVI and nZVI/BC could effectively promote the transformation of more accessible Cr into less accessible forms, thereby reducing the toxicity and bioavailability of Cr(VI) (Lyu et al. 2018).

3.2.3 The effect of different materials on soil pH, SOM, and CEC

Detecting the changes in soil properties is a significant part of evaluating the remediation ability of nZVI/BC. The soil pH increased after remediation by the three materials. Compared with CK (pH: 6.73), the pH of BC, nZVI, and nZVI/BC treatments increased by 0.17, 0.65, and 0.64, respectively (under a dose of 8 g/kg for nZVI/BC) (Fig. 4a). Moreover, the pH values increased with higher material dosage. The impact of BC on soil pH depended on the acidity or alkalinity of BC (Wang et al. 2021). In our research, the pH values of BC is 8.52, which was helpful for increasing the pH of soil. Moreover, compared with alkaline soil, the acidic soil had lower buffering capacity, such that the soil pH was increased after addition of BC (Baragaño et al. 2020). As for nZVI or nZVI/BC particles, during the reaction between Fe^0 and Cr(VI), H^+ could be consumed, thereby increasing the pH values, which is in agreement with other studies (Gil-Díaz et al. 2016; Vasarevičius et al. 2019).

With the dose of 2, 4, and 8 g/kg, the SOM contents were 11.81, 11.94, and 11.36 g/kg after nZVI/BC treatment, respectively, which were higher than those of CK (10.72 g/kg) (Fig. 4b). The use of BC significantly increased soil SOM contents. This observation was consistent with a previous work (Wang et al. 2021). Being a material with high carbon content, BC can significantly increase the total organic carbon of the soil (Herath et al. 2017). Meanwhile, the small organic molecules can be adsorbed during the remediation process, thus promoting the formation of SOM (Liang et al. 2009). The application of nZVI did not affect the SOM content in our study.

Figure 4c shows the changes in CEC values before and after treatment by the three materials. The application of BC increased the soil CEC at a higher dosage. Compared with CK (6.33 cmol/kg), the soil CEC values were 7.29, 8.73, and 8.86 cmol/kg with three different doses of BC. The usage of nZVI/BC also increased the CEC values. While for nZVI treatments, the CEC values did not change. The negative charge generated by the abundant oxygen-containing functional groups on the surface of BC increases the adsorption capacity of cations, thereby increasing the CEC values (Randolph et al. 2017). The results showed that the application of BC and nZVI/BC could change the soil properties in a short time. However, these changes were mainly related to the physicochemical properties of BC.

3.3 Characterization of remediation materials

In our research, the nZVI/BC particles were separated by using the magnetic properties of nanocomposites. The separation efficiency was about 60%. By comparing the SEM–EDS images of BC (Fig. 5a, b) and nZVI/BC (Fig. 5c, d), we found that the pore structure of BC was well developed and contained a variety of elements, which was related to the abundance of elements in the MSS. NZVI nanoparticles were dispersed uniformly on the BC surface. As a carrier, BC could improve the reduction and adsorption ability of nZVI by alleviating the agglomeration effect of nanoparticles (Shang et al. 2017). However, in our research, some nZVI particles were still aggregating in chains, which might be explained by the excessive loading of nZVI on the surface of BC (nZVI loads: 407.4 mg/g). After incubation, we could see that the nZVI content on the surface of BC was significantly reduced, which was caused by the release of iron in soil. Moreover, some flocculent clusters covered on the nZVI surface, which was related to the generation of (hydr)oxide of Cr(III) (Fe(III)) during remediation process (Zhou et al. 2015). EDS analysis also confirmed the presence of Cr after incubation (Fig. 5f), which was consistent with the fraction analysis.

As shown in Fig. 6a, the typical peak of Fe^0 ($2\theta = 44.6°$) revealed the successful loading of nZVI. Compared with nanocomposites, the unsupported BC showed several peaks

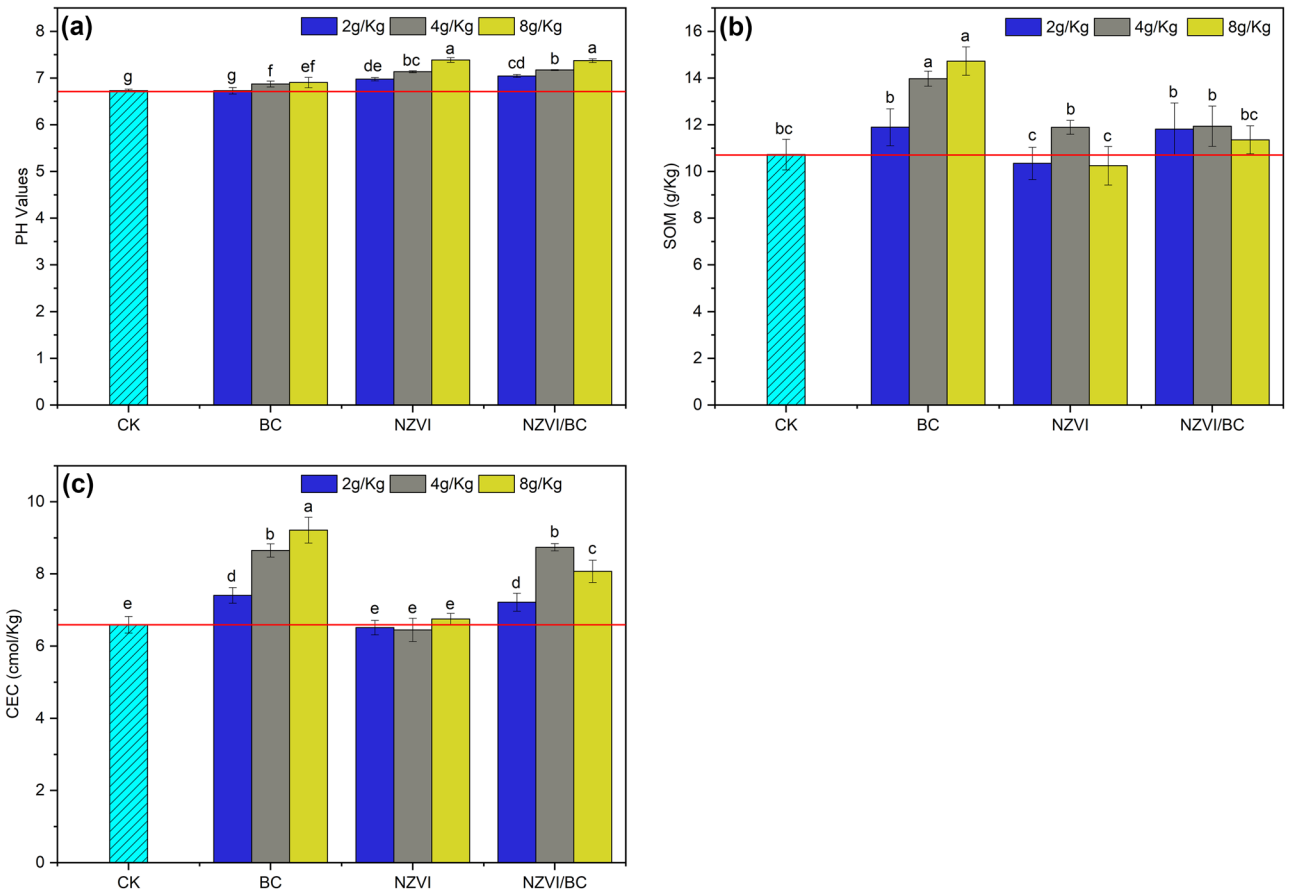

Fig. 4 The PH values (**a**), SOM contents (**b**), and CEC values (**c**) in soil

of SiO_2, which was related to the composition of MSS, while these peaks were hardly be observed after nZVI loading. This phenomenon indicated that the nZVI were made of crystals and covered the surface of BC (Fu et al. 2013).

As shown in Fig. 6b, the broad peak at around 3420 cm^{-1} represents O–H structure for both samples (Bing et al. 2018). The peak appeared at 1638 cm^{-1} reflects the stretching vibrations of C = O or the vibration of aromatic C = C (Amezquita-Garcia et al. 2013; Xu et al. 2017). The small peak at about 1380 cm^{-1} could be attributed to the C = C stretching in aromatic ring carbons (Peng et al. 2016). The peak appeared at 1070 cm^{-1} and 1110 cm^{-1} could be assigned to C–O stretching vibration. However, the change in wave number might be owed to the attachment of oxygen with adjacent carbon elements during synthesis of nZVI/BC (Lu et al. 2021). Moreover, it was worth noting that the –OH groups in nZVI/BC were wider and stronger than those of BC, which could be explained by the combination of iron with oxygen elements after nZVI loading (Xue et al. 2018). Both C–O and –OH groups played a significant role in adsorption of Cr(VI) and surface complexation of Cr(III), which was helpful for Cr immobilization (Lyu et al. 2017).

3.4 Probable reaction mechanism between Cr(VI) and nZVI/BC in soil system

The XPS analysis was applied for evaluating the reaction mechanism between Cr(VI) and nZVI/BC. The wide-scan XPS analysis showed that the Cr species (at about 580.0 eV) appeared on nZVI/BS surface after 30-day incubation (Fig. 7a). The area percentage of Cr 2p after incubation was 0.73%, while no Cr species were detected before remediation. As we can see from Fig. 7b, the peaks observed at 529.0 eV and 530.3 eV corresponded to the binding energies of O^{2-} (Wang et al. 2020; Yin et al. 2014). However, a slight shift occurred with two corresponding peaks, which was due to the oxygen-containing functional groups were involved in the formation of Cr(III)/Fe(III) oxides/hydroxides (Wang et al. 2020). The peak appeared at about 531.2 eV could be assigned to the OH groups (Yin et al. 2014), which was consistent with the FTIR analysis. As shown in Fig. 6c, the peaks appeared at about 725.0 and 711.0 eV were related to the binding energies of Fe (hydr)oxide (Geng et al. 2009). The XPS spectra for Fe 2p3/2 could be divided into two peaks at 709.5 and 711.2 eV, which correspond to the

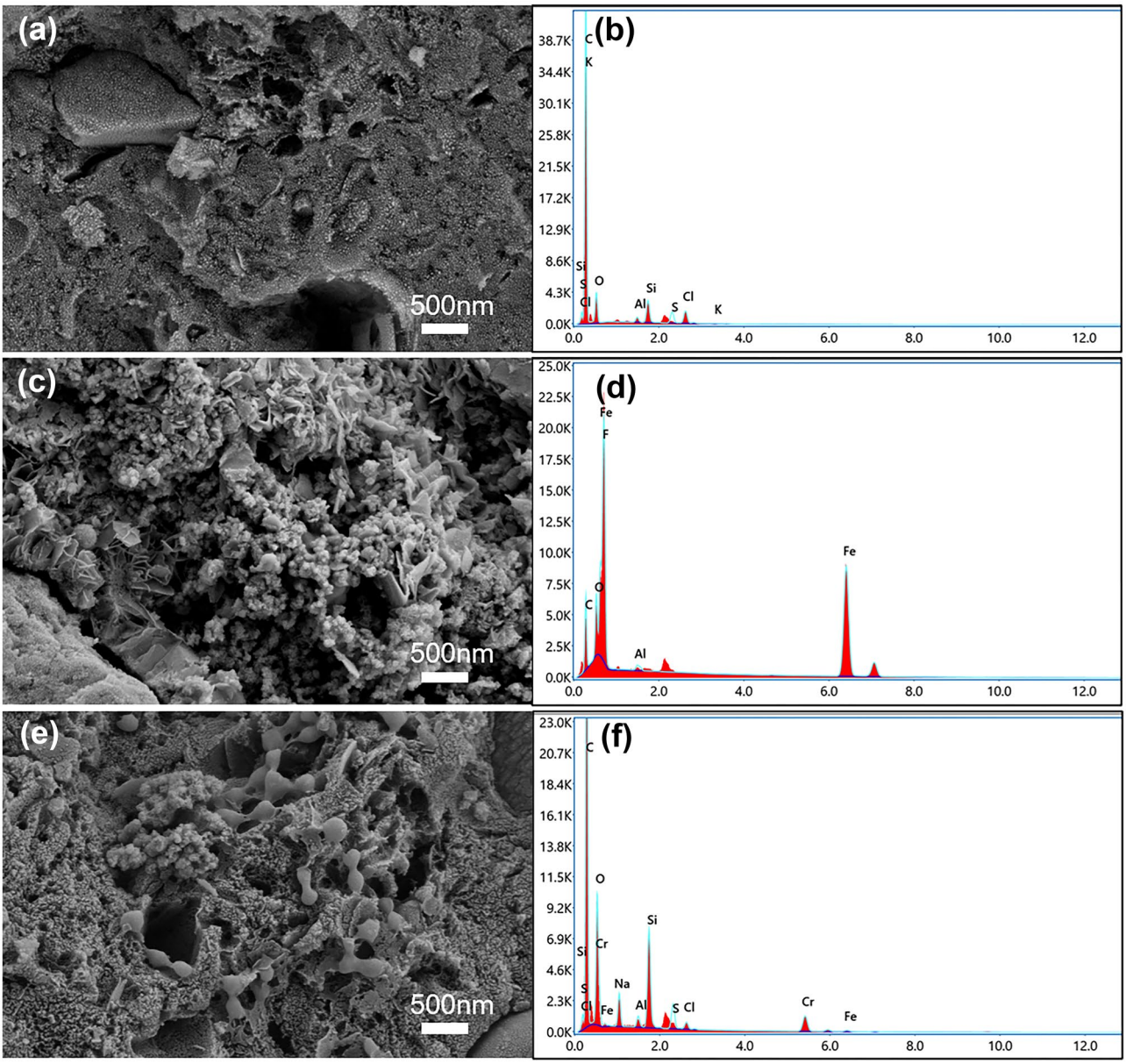

Fig. 5 SEM–EDS images of BC (**a**, **b**), nZVI/BC (**c**, **d**), and nZVI/BC after incubation (**e**, **f**)

binding energies for Fe^{2+} and Fe^{3+}, respectively (Bae et al. 2016). The peak which assigned to Fe^0 (at about 706.0 eV) could not be observed in our research. This phenomenon could be explained by the oxidation that occurred on the surface of the nZVI (Zhou et al. 2015). However, the surface oxidation endowed nZVI with a special core–shell structure, which enables it to possess strong adsorption, coordination, and reduction capabilities (Yan et al. 2010). The peak at 718.2 eV was assigned to the shakeup satellite overlap in oxidized iron (2p3/2) (Li and Zhang 2007). The Cr 2p3/2 proportion was composed of two peaks at 578.1 and 576.0 eV (Fig. 7d), which assigned to the Cr(VI) and Cr(III) (Lv et al. 2012). The result suggested that both adsorption and reduction were included in the remediation process, which was also in agreement with our experimental result.

Compared with aqueous solution, the process of material migration and transformation in soil system was more complicated, but the reaction mechanism between nZVI/BC and Cr(VI) was almost the same in both water and soil environment (Fig. 8). Combined with the results of Cr fraction analysis, the probable reaction mechanism between Cr(VI) and nZVI/BC could be summarized as follows: as a material with a well-developed porous structure and rich in surface functional groups, BC has strong adsorption capacity for Cr(VI). Moreover, it also provided conditions for the uniform loading of nZVI particles, thereby increasing the reaction site. NZVI

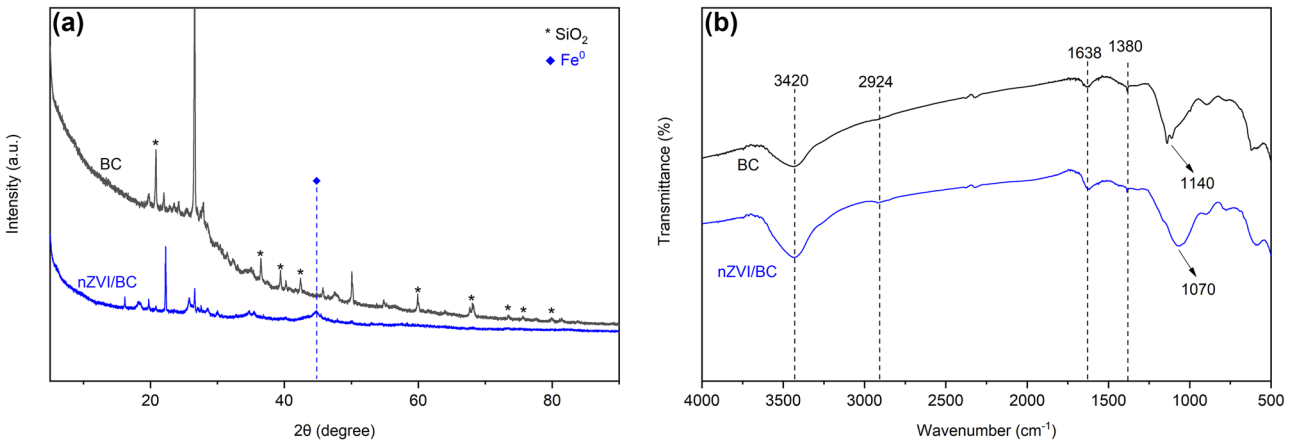

Fig. 6 XRD patterns (**a**) and FTIR spectra (**b**) of BC and nZVI/BC

mainly contributed to the reduction of Cr(VI) through redox reaction, and the Fe^{2+} generated by oxidation also played a role in Cr(VI) reduction (Eqs. (2) and (3)). The newly generated Cr(III) could combine with Fe(III) and co-precipitated on the surface of the nanomaterials (Eq. (4)), or precipitated in the form of $Cr(OH)_3$ (Eq. (5)). Plus, a normalization reaction could occur between nZVI and Fe^{3+} (Eq. (6)), thus making the treatment process more thorough.

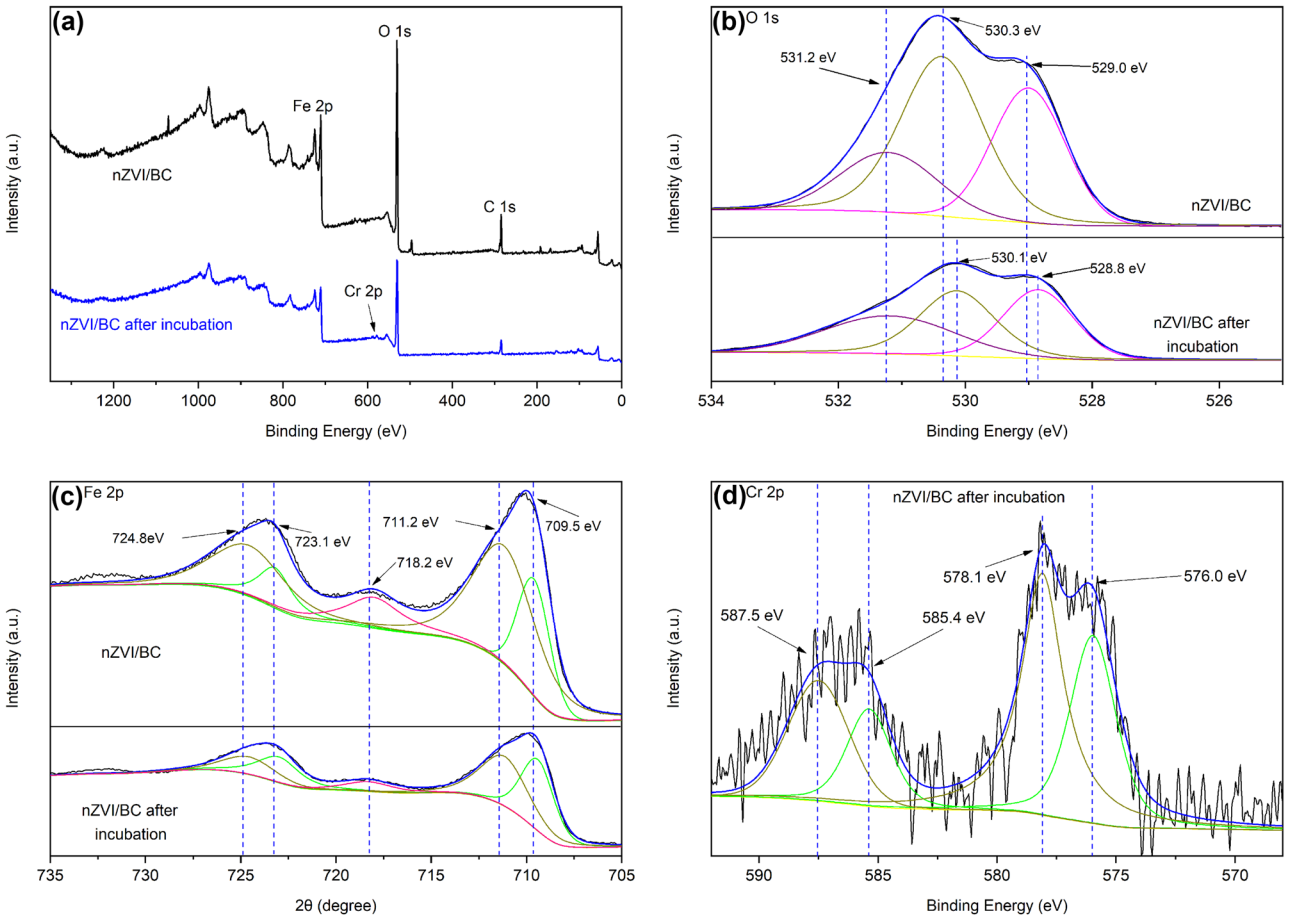

Fig. 7 Wide-scan XPS analysis of nZVI/BC before and after 30-day incubation (**a**), narrow scan of O 1 s (**b**) and Fe 2p (**c**) before and after incubation, and narrow scan of Cr 2p (**d**) after incubation

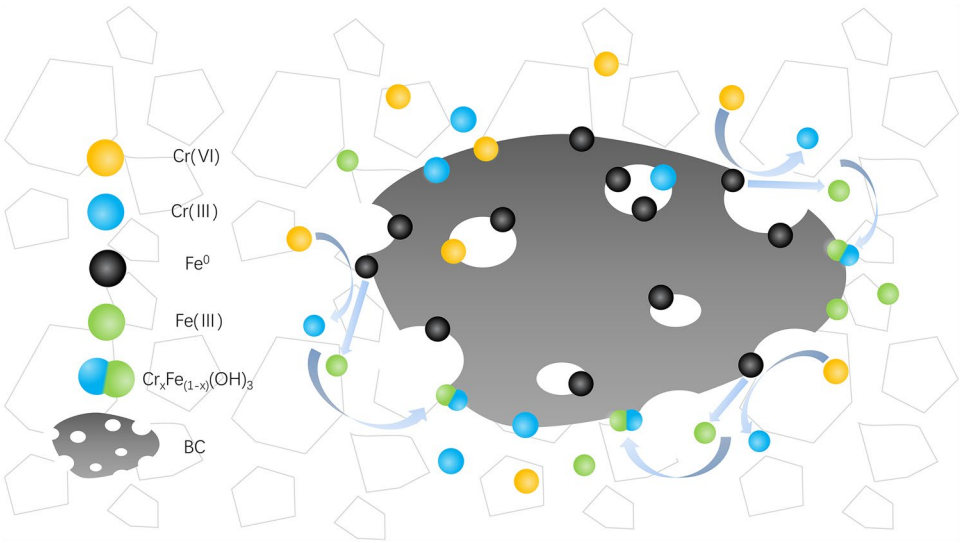

Fig. 8 The reaction mechanism between Cr(VI) and nZVI/BC in soil system

$$Cr_2O_7^{-2} + 3Fe^0 + 14H^+ \rightarrow 3Fe^{2+} + 2Cr^{3+} + 7H_2O \quad (2)$$

$$Cr_2O_7^{-2} + 6Fe^2 + 14H^+ \rightarrow 6Fe^{3+} + 2Cr^{3+} + 7H_2O \quad (3)$$

$$XCr^{3+} + (1-X)Fe^{3+} + 3H_2O \rightarrow Cr_xFe_{(1-x)}(OH)_3 \downarrow + 3H^+ \quad (4)$$

$$Cr^{3+} + 3OH^- \rightarrow Cr(OH)_3 \downarrow \quad (5)$$

$$2Fe^{3+} + Fe^0 \rightarrow 3Fe^{2+} \quad (6)$$

4 Conclusion

The research investigated the remediation efficiency of nZVI/BC on Cr(VI)-polluted soil. The nZVI/BC particles which were prepared by liquid phase reduction method exhibited superior remediation capacity than bare nZVI and BC, with significant reductions in TCLP-leachable Cr(VI) concentrations. Moreover, the addition of nZVI/BC effectively transformed the fraction of Cr from unstable to stable, thereby reducing the toxicity of Cr. The addition of nZVI could not affect the soil properties in a short term. However, as a carbon-rich solid, BC contained a variety of functional groups, with high specific surface area, which is beneficial to properties of the soil. The reduction and adsorption process might be the main reaction mechanism for Cr(VI) immobilization by nZVI/BC. Overall, the nZVI/BC particles combined the advantages of BC and nZVI, which was more suitable for the immobilization of Cr(VI) in soil.

Author contribution All authors contributed to the study conception and design. Material preparation, data collection, and analysis were performed by XZ, YL, and YL. The first draft of the manuscript was written by GF and all authors commented on previous versions of the manuscript. All authors read and approved the final manuscript.

Funding This work was supported by The National Key Research and Development Project Subject (ZX20200121).

Data availability The data presented in this study are available on request from the corresponding author. The data are not publicly due to privacy.

Declarations

Conflict of interest The authors declare no competing interests.

References

Ahmed MMM, Balal Y, Ubaid AM, Chen D, Qumber A, Muhammad A, Xiaoe Y (2021) In situ synthesis of micro-plastics embedded sewage-sludge co-pyrolyzed biochar: implications for the remediation of Cr and Pb availability and enzymatic activities from the contaminated soil. J Clean Prod 302

Amezquita-Garcia HJ, Razo-Flores E, Cervantes FJ, Rangel-Mendez JR (2013) Activated carbon fibers as redox mediators for the increased reduction of nitroaromatics. Carbon 55:276–284

Bae S, Gim S, Kim H, Hanna K (2016) Effect of NaBH 4 on properties of nanoscale zero-valent iron and its catalytic activity for reduction of p-nitrophenol. Appl Catal B 182:541–549

Baragaño D, Alonso J, Gallego JR, Lobo MC, Gil-Díaz M (2020) Zero valent iron and goethite nanoparticles as new promising remediation techniques for As-polluted soils. Chemosphere 238

Bing Z, Xinyang X, Fanqiang Z, Haibo L, Xi C (2018) The hierarchical porous structure bio-char assessments produced by co-pyrolysis of municipal sewage sludge and hazelnut shell and Cu(II) adsorption kinetics. Environ Sci Pollut Res 25:19423–19435

Devi P, Saroha AK (2014) Synthesis of the magnetic biochar composites for use as an adsorbent for the removal of pentachlorophenol from the effluent. Bioresour Technol 169:525–531

Fu F, Ma J, Xie L, Tang B, Han W, Lin S (2013) Chromium removal using resin supported nanoscale zero-valent iron. J Environ Manage 128:822–827

Geng B, Jin Z, Li T, Qi X (2009) Preparation of chitosan-stabilized Fe 0 nanoparticles for removal of hexavalent chromium in water. Sci Total Environ 407:4994–5000

Geng H-X, Wang L (2019) Cadmium: toxic effects on placental and embryonic development. Environ Toxicol Pharmacol 67:102–107

Gil-Díaz M, Diez-Pascual S, González A, Alonso J, Rodríguez-Valdés E, Gallego JR, Lobo MC (2016) A nanoremediation strategy for the recovery of an As-polluted soil. Chemosphere 149:137–145

Herath I, Iqbal MCM, Al-Wabel MI, Abduljabbar A, Ahmad M, Usman ARA, Ok YS, Vithanage M (2017) Bioenergy-derived waste biochar for reducing mobility, bioavailability, and phytotoxicity of chromium in anthropized tannery soil. J Soils Sediments 17:731–740

Kotaś J, Stasicka Z (2000) Chromium occurrence in the environment and methods of its speciation. Environ Pollut 107:263–283

Li XQ, Zhang WX (2007) Sequestration of metal cations with zerovalent iron nanoparticles – a study with high resolution X-ray photoelectron spectroscopy (HR-XPS). J Phys Chem C 111:6939–6946

Liang B, Lehmann J, Sohi SP, Thies JE, O'Neill B, Trujillo L, Gaunt J, Solomon D, Grossman J, Neves EG, Luizão FJ (2009) Black carbon affects the cycling of non-black carbon in soil. Org Geochem 41:206–213

Liu T, Rao P, Lo IMC (2009) Influences of humic acid, bicarbonate and calcium on Cr(VI) reductive removal by zero-valent iron. Sci Total Environ 407:3407–3414

Liu X, Zhang S, Zhang X, Guo H, Lou Z, Zhang W, Chen Z (2022) Cr(VI) immobilization in soil using lignin hydrogel supported nZVI: immobilization mechanisms and long-term simulation. Chemosphere 305

Lu Y, Xie Q, Tang L, Yu J, Wang J, Yang Z, Fan C, Zhang S (2021) The reduction of nitrobenzene by extracellular electron transfer facilitated by Fe-bearing biochar derived from sewage sludge. J Hazard Mater 403

Lv X, Xu J, Jiang G, Tang J, Xu X (2012) Highly active nanoscale zero-valent iron (nZVI)–Fe 3 O 4 nanocomposites for the removal of chromium(VI) from aqueous solutions. J Colloid Interface Sci 369:460–469

Lyu H, Tang J, Huang Y, Gai L, Zeng EY, Liber K, Gong Y (2017) Removal of hexavalent chromium from aqueous solutions by a novel biochar supported nanoscale iron sulfide composite. Chem Eng J 322:516–524

Lyu H, Zhao H, Tang J, Gong Y, Huang Y, Wu Q, Gao B (2018) Immobilization of hexavalent chromium in contaminated soils using biochar supported nanoscale iron sulfide composite. Chemosphere 194:360–369

Manning BA, Kiser JR, Kwon H, Kanel SR (2007) Spectroscopic investigation of Cr(III)- and Cr(VI)-treated nanoscale zerovalent iron. Environ Sci Technol 41:586–592

Megharaj M, Avudainayagam S, Naidu R (2003) Toxicity of hexavalent chromium and its reduction by bacteria isolated from soil contaminated with tannery waste. Curr Microbiol 47:51–54

Miao C, Jian Z, Yaozong C, Peng H, Fang C, Xu W, Jinye L, Chunyao G, Dongli H, Ke Z, Min G, Jianyu Z (2021) An efficient, economical, and easy mass production biochar supported zero-valent iron composite derived from direct-reduction natural goethite for Cu(II) and Cr(VI) remove. Chemosphere 285:131539–131539

Peng C, Zhai Y, Zhu Y, Xu B, Wang T, Li C, Zeng G (2016) Production of char from sewage sludge employing hydrothermal carbonization: char properties, combustion behavior and thermal characteristics. Fuel 176:110–118

Randolph P, Bansode RR, Hassan OA, Rehrah D, Ravella R, Reddy MR, Watts DW, Novak JM, Ahmedna M (2017) Effect of biochars produced from solid organic municipal waste on soil quality parameters. J Environ Manage 192:271–280

Ruili G, Hongqing H, Qingling F, Zhenhua L, Zhiqiang X, Umeed A, Jun Z, Yonghong L (2020) Remediation of Pb, Cd, and Cu contaminated soil by co-pyrolysis biochar derived from rape straw and orthophosphate: speciation transformation, risk evaluation and mechanism inquiry. Sci Total Environ 730

Sarwar N, Imran M, Shaheen MR, Ishaque W, Kamran MA, Matloob A, Rehim A, Hussain S (2017) Phytoremediation strategies for soils contaminated with heavy metals: modifications and future perspectives. Chemosphere 171:710–721

Shang J, Zong M, Yu Y, Kong X, Du Q, Liao Q (2017) Removal of chromium (VI) from water using nanoscale zerovalent iron particles supported on herb-residue biochar. J Environ Manage 197

Shi L-n, Lin Y-M, Zhang X, Chen Z-l (2011) Synthesis, characterization and kinetics of bentonite supported nZVI for the removal of Cr(VI) from aqueous solution. Chem Eng J 171:708–715

Singh R, Misra V, Singh RP (2011) Synthesis, characterization and role of zero-valent iron nanoparticle in removal of hexavalent chromium from chromium-spiked soil. J Nanopart Res 13:4063–4073

Sneath HE, Hutchings TR, Leij FAAMd (2013) Assessment of biochar and iron filing amendments for the remediation of a metal, arsenic and phenanthrene co-contaminated spoil. Environ Pollut 178:361–366

Su H, Fang Z, Tsang PE, Fang J, Zhao D (2016) Stabilisation of nanoscale zero-valent iron with biochar for enhanced transport and in-situ remediation of hexavalent chromium in soil. Environ Pollut 214:94–100

Tan X-f, Liu Y-g, Gu Y-l, Xu Y, Zeng G-m, Hu X-j, Liu S-b, Wang X, Liu S-m, Li J (2016) Biochar-based nano-composites for the decontamination of wastewater: a review. Bioresour Technol 212:318–333

Tu C, Wei J, Guan F, Liu Y, Sun Y, Luo Y (2020) Biochar and bacteria inoculated biochar enhanced Cd and Cu immobilization and enzymatic activity in a polluted soil. Environ Int 137

Vasarevičius S, Danila V, Paliulis D (2019) Application of stabilized nano zero valent iron particles for immobilization of available Cd2+, Cu2+, Ni2+, and Pb2+ ions in soil. Int J Environ Res 13:465–474

Wang Y, Zheng K, Zhan W, Huang L, Liu Y, Li T, Yang Z, Liao Q, Chen R, Zhang C, Wang Z (2021) Highly effective stabilization of Cd and Cu in two different soils and improvement of soil properties by multiple-modified biochar. Ecotoxicol Environ Saf 207:111294–111294

Wang Z, Chen G, Wang X, Li S, Liu Y, Yang G (2020) Removal of hexavalent chromium by bentonite supported organosolv lignin-stabilized zero-valent iron nanoparticles from wastewater. J Clean Prod 267

Xi C, Guangjian F, Haibo L, Yinghua L, Ran Z, Yu H, Xinyang X (2021) Nanoscale zero-valent iron particles supported on sludge-based biochar for the removal of chromium (VI) from aqueous system. Environ Sci Pollut Res 29:3853–3863

Xu X, Zhao B, Sun M, Chen X, Zhang M, Li H, Xu S (2017) Co-pyrolysis characteristics of municipal sewage sludge and hazelnut shell by TG-DTG-MS and residue analysis. Waste Manage 62:91–100

Xu Y, Zhao D (2007) Reductive immobilization of chromate in water and soil using stabilized iron nanoparticles. Water Res 41(10):2101–2108

Xue W, Huang D, Zeng G, Wan J, Zhang C, Xu R, Cheng M, Deng R (2018) Nanoscale zero-valent iron coated with rhamnolipid as an effective stabilizer for immobilization of Cd and Pb in river sediments. J Hazard Mater 341:381–389

Yan W, Herzing AA, Kiely CJ, Zhang W-x (2010) Nanoscale zero-valent iron (nZVI): aspects of the core-shell structure and reactions with inorganic species in water. J Contam Hydrol 118:96–104

Yin X, Liu W, Ni J (2014) Removal of coexisting Cr(VI) and 4-chlorophenol through reduction and Fenton reaction in a single system. Chem Eng J 248:89–97

Zhou X, Lv B, Zhou Z, Li W, Jing G (2015) Evaluation of highly active nanoscale zero-valent iron coupled with ultrasound for chromium(VI) removal. Chem Eng J 281:155–163